Sensor Temperature for a Low-Power Low-Voltage Self-Powered System Using Vibration Scavenging.

J.COLOMER, A.SAIZ,P.MIRIBEL,J.MAÑA,J.BRUFAU,M.PUIG,J.SAMITIER
Electronics Department. Instrumentation and Communications Systems Lab (SIC)
University of Barcelona
c/ Marti i Franquès,1 Facutat de Física, 08028 Barcelona
SPAIN

www.el.ub.es

Abstract: - This paper presents the conception of a Smart Low Power Temperature Sensor which is powered using ambient vibration energy. It is presented the architecture of the conception of the sensor to be implemented. This power system will be the main part of the power stage for a self-powered micro temperature sensor inside a distributed sensor network where accessibility to human being operators is very difficult. The oriented application of this system is to sense the temperature in harsh environments or when accessibility is limited to human operators. A full analysis of the sensor is presented.

Key-Words: - Scavenging, Vibrational sources, Low-Power circuits, bandgap reference, temperature sensor.

1 Introduction

The evolution of new self-powered portable devices that integrate several functions is growing rapidly over these last years, thanks to the advances in the semiconductor's technology in terms of transistor size reduction. A great variety of new low power compact devices as wireless ad-hoc networks, biomedical electronics, and cell-phones have been developed [1][2]. A very important bottleneck for portable devices is that a battery is used. Thanks to the development of the low power electronics, the field of power scavenging has renewed the interest of the engineers, increasing the life-time of battery powered systems, or looking for systems which are based on alternative power sources, like ambient vibration, to provide infinite life systems[3][4].

The conception of the system based on a power solution that harvests ambient vibration energy is presented. Section 2 develops the electrical modelization of the piezoelectric generator. In section 3, it is presented the conception of the full system. In section 4, are presented the main circuits that define the whole system, Finally the conclusions of the work and future implementations are commented.

2 The Vibration Energy Source

The Piezoelectric generator used is based on the Quick Pack QP20W (Midé Technology Corporation, Medford, MA, USA). The Quick Pack is a composite beam made of 2 piezoelectric layers working as a bimorph, with an intermediate layer based on Polyimide. This composite beam is then located with one end clamped to a vibrating body and the other end remaining free. The vibrations forced at the clamped end are propagated along the cantilever beam. This wave generates an induced strain in the membrane, which at the same time produces an electrical charge.

In order to be able to recover this energy a Lumped Electrical Model compatible with Spectre software has been developed. The model is based on the Modal analysis of piezoelectric Euler-Bernoulli beam equation [5]. Solving the beam equation for the first resonance mode, and considering the equivalence between the equations defining a mechanical system, and the equations defining an electrical circuit, an electromechanical equivalent circuit is created. Each of the electrical components, based on resistances, capacitors and inductors, have been defined by means of the beam geometrical and material parameters. Due to the composite nature of the material some of these parameters are experimentally identified. In order to increase the current capability of the power source, some PZT's are placed in parallel allowing the system to obtain a higher current. Different simple PZT generators are connected in parallel creating an array of generators. This array is then connected to the power conditioning circuitry to load the supercapacitor.

3 Conception of the powered system

At this stage of the system's conception, just one powering source is analyzed. In the near future we would like to combine the vibration source with the

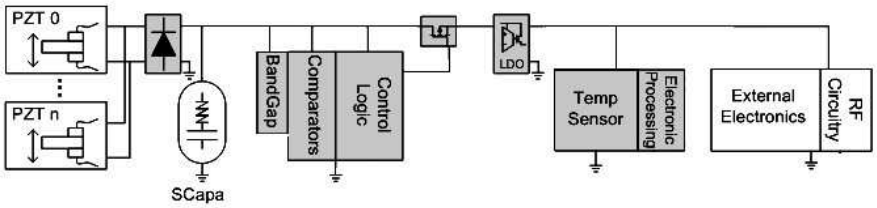

Fig 1. Self-powered SiP proposed with LDO.

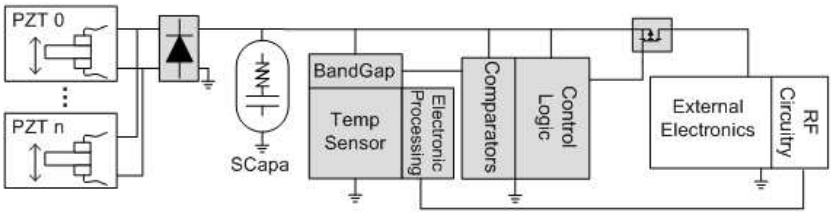

Fig 2. Self-powered SiP proposed (grey zone represents IC implementation).

wireless communication between the tag and the reader. In this way the system will have to independent powering sources. Then, the system will not rely on just one power source. Working with the first solution, based on the vibration scavenging, the circuit modules are presented. The AC signal that is generated by the piezoelectric power generator must be rectified to have a DC signal, with some ripple. This voltage charges a supercapacitor (SCAP). This situation defines de conception of an integrated rectifier. At this stage a non-synchronous solution has been adopted because of the complexity, in terms of area and consumption, of a synchronous rectifier. Future works would be oriented to implement this solution. From the DC non-regulated voltage arises an important question. Would be interesting to place a linear regulator or not, after the supercapacitor? One solution it is based on the use of a linear low-dropout regulator (LDO). When the DC voltage at the SCAP (Csc), reaches a maximum value (Vout,max),

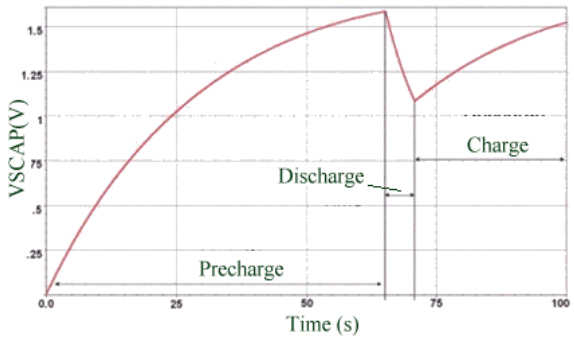

Fig 3. Self-Powered System for a particular case.

$$\Delta E(J) = \frac{1}{2}\ C_{SC}\ (Vout,\max)^2 - \frac{1}{2}\ C_{SC}\ (Vout,\min)^2 \quad (1)$$

a PMOS switch is switched-on in such a way that the LDO starts to regulate. This regulated voltage is used to bias the integrated temperature sensor, some integrated processing electronics, an also the RX/TX electronics, which in our case and at this stage are conceived to be external. At this point the SCAP is discharged, delivering the power needed for all the electronics. This step of discharge ends at a minimum voltage (Vout,min), which is defined by the minimum voltage available for the LDO to assure the regulated output voltage. This conception is depicted in Fig.1. The system then works between to phases. One is the charge phase; that is, the SCAP is charged up to Vout,max. Then, when this voltage is reached starts the discharge phase up to Vout,min. The power conditioning circuit controls these phases. This architecture has been analyzed. The power level needed to source, mainly, the RX/TX, and the time to assure the right communication fixes the amount of energy that must be delivered by the SCAP during the discharge phase. In (1) is presented the equation that allows sizing the SCAP value.

The values used to size the piezoelectric source and the capabilities of the used technology (Hcmos9gp 0.13µm, from ST Microelectronics) are a maximum DC voltage of 1.8V. An LDO capable to regulate a voltage level of 1.2V and a DC load current up to 2.5mA has been designed. In this way the system is able to define a regulated DC voltage for the temperature sensor and the rest of the electronics, integrated or external. The LDO is based on a bandgap reference, and the powering control needs some comparators and logic control. The same LDO to handle with the load needs implies area and power consumption. But then another question arose. The LDO can be removed? This question then defines the second architecture, which is depicted in Fig.2.

The second solution rectifies the AC signal produced by the piezoelectric source and charges a huge capacitor (SCAP), using an unregulated DC voltage. Furthermore, this unregulated voltage biases the whole electronics, as is depicted in Fig.3. The idea is that the full available range of voltage from the supercapacitor is useful for the electronics, and the use of a huge LDO is not necessary, saving energy. The logic control works as mentioned previousl = 10 mF, and a load condition equivalent of a power of 1.125 mW is presented to show the performance of the power conditioning circuit. The discharge ends y and it controls two voltage levels, but in this case, defined by the suitable voltage range for the electronics. This has been the selected option to develop the system. In Fig. 3, a particular case study with a C_{SC} when the voltage arrives to the value of 1.1V (Vout,min), switching off the PMOS transistors. Then the capacitor charges again up to the value of 1.6V. During the discharge phase, the temperature must be sensed, and then the value must be processed to be sent by the communications circuitry. In the next section we present the electronics involved, in more detail, taking special attention to the temperature sensor.

4 The involved electronics

In this section we present the electronics to be integrated in a first IC to test the selected architecture.

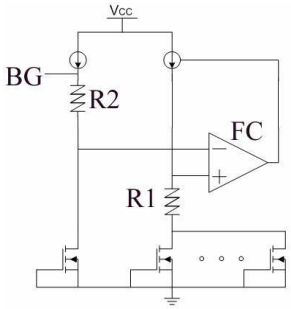

Fig 4. Bandgap reference architecture.

4.1 The Integrated Rectifiers

Since the PZT generator supplies an AC voltage a rectification stage is needed. Two different rectifiers [3][4] based on the diode bridge configuration have been tested. The first one based on NMOS transistors [3], and the second one based on PMOS transistors[4]. From the simulations, the efficiency of both architectures achieves a 70%, although the PMOS rectifier presents a better behavior with efficiency near 72%. In spite of this better efficiency, the NMOS rectifier has been selected due to its reduced size. The PMOS rectifier is 10 times higher than the NMOS rectifier.

4.2 The Bandgap reference circutry

A bandgap reference circuit is needed to define the window of voltages for the power management circuitry. The bandgap reference architecture is based on the voltage summing solution [6][7], depicted in Fig.4. In classical designs the bandgap is based on parasitic diodes related to bipolar transistors. In the used technology it is not possible to have access to bipolar transistors. A full reference circuit based just in MOSFET transistors has been designed based on [8]. The exponential characteristic of the current-to-voltage through the typical diode connected bipolar transistors is now defined by MOSFET transistors, in a shorter voltage range. This current-to-voltage enables us to have a current, which is proportional to the temperature (PTAT).

The bandgap reference voltage is obtained by summing in an appropriate way, the voltage drop in one MOSFET, which follows a conversely proportional to temperature relationship (CTAT), and the drop in a resistor where is injected the PTAT current.

Full simulations of the bandgap reference circuit have been done. The variations of the regulated voltage in terms of the voltage and the mobility have been done. The bandgap must assure a reference voltage that must have a high PSRR. Taking into account that the circuit will see the variations of voltage at the SCAP, between Vout,max and Vout,min, the reference voltage must be very well defined. In Fig.5 are depicted the simulations of the reference voltage for input voltages from the defined Vout,max = 1.8V, to a critical case of Vout,min= 1.0 V, and also for the different electrical models, defined by the typical case (TYP) for the mobility's, resistance values, capacitors, etc, the fast case (FFA), and the slow case (SSA). The average reference voltage (BG), for the typical case (TYP), is 513mV, with a maximum variation of ± 2.5mV in the full range of temperatures (from 0ºC to 100ºC), and for a variation in the power supply from 1.0V to 1.8V. In the case of the slow case the average value is 542mV, and for the fast case (FFA), the average value is 477mV.

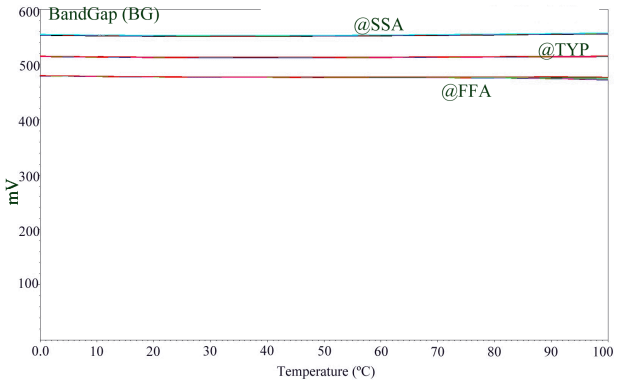

Fig 5. Bandgap voltages.

4.3 The Temperature Sensor

This is an implementation where the system is not looking for a high level of accuracy like in [9]. Nor healthcare applications, where reduced temperature ranges but higher accuracy is needed, will be covered with this first design. For this reason, a single solution has been adopted.

The designed solution it is based on the use of the same bandgap reference circuit and the single temperature sensor presented in [10], and based on [11]. The gate-source voltage (V_{GS}), of an NMOS transistor with an invariant drain-source current (I_{DS}),

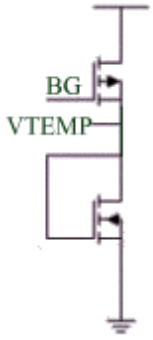

Fig6. Schematic of the temperature sensor.

injected through it, defines a linear relationship between V_{GS} and the temperature. The schematic of the sensor is depicted in Fig.6. Using the bandgap reference voltage to bias the PMOS gate terminal we can achieve a first temperature sensor approach. But taking into account that the bandgap reference, and also the temperature sensor, are connected to a variable voltage source, defined by values of the charge phase and discharge phase of the power management circuitry (Vout,max and Vout,min), a modification in the bandgap circuitry must be adopted. In Fig.7 we have depicted the performance

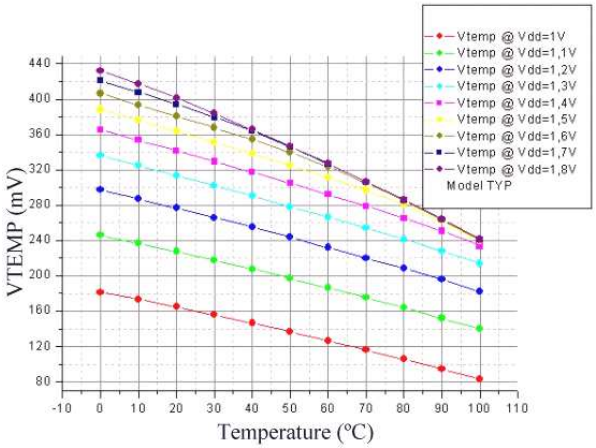

Fig 7. Temperature response without preregulator. @ TYP

of the temperature sensor when changes of the bias voltage are present, for the typical case (TYP). The error present between extreme voltages is unacceptable. The main source of error is the variation of the bias. Then, two options where analyzed. Both solutions are based on the use of a preregulator for the input voltage. Following this solution the systems looks for a better voltage at the sensor bias. The first solution is based on the design of a pre-regulated pseudo-supply like in [12]. In this design the current source used for the bandgap is used also to bias the preregulator. The variations of the temperature sensor were too important for the extreme mobility conditions. Then, a second solution was adopted, and it is based on a small and low power LDO. This LDO, in this case, just is needed to regulate the voltage at the temperature sensor. The power consumption by the sensor is very low, just few µW instead of the case of architecture depicted in Fig.2, where the removed LDO must be designed to work with DC levels of 2.5mA. The power consumption of the preregulator, bandgap and for the temperature sensor is presented in Table 1.

Vdd (V)	LDO		BG		Sensor	
	I (*nA*)	P_{con} (*nW*)	*I* (*µA*)	P_{con} (*µW*)	*I* (*pA*)	P_{con} (*nW*)
1	102	**102**	6,27	**6,27**	657	**0.657**
1,1	101	**112.2**	6,274	**6,901**	661	**0.727**
1,2	101	**121.2**	6,277	**7.532**	664	**0.796**
1,3	102	**131.3**	6,28	**8.16**	666	**0.866**
1,4	102	**142.8**	6,283	**8.796**	668.2	**0.9355**
1,5	102	**153**	6,285	**9.428**	669.7	**1.0054**
1,6	102	**163.2**	6,289	**10.064**	671	**1.074**
1,7	102	**173.4**	6,292	**10.696**	672	**1.142**
1,8	102	**183.6**	6,296	**11.333**	672.7	**1.2109**

Table 1. Power Dissipation

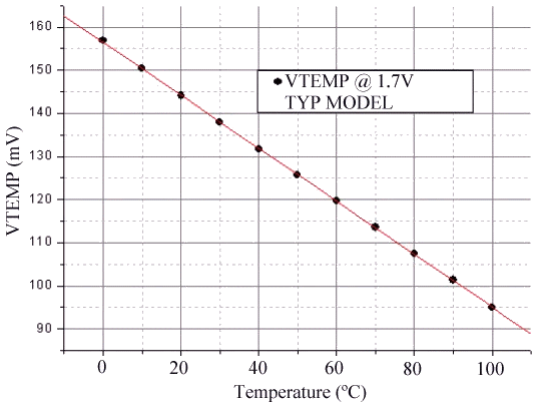

Fig 8. Fit line @ 1,7V for the TYP Case.

The sensor must have a very linear response, and the variation between Vout,max and Vout,min must be limited. During the discharge phase the sensor makes the lecture. During this time, just few seconds, it is presumed that the temperature variation is very small. The defined process of lecture is as follows. When the discharge phase starts, the temperature is sensed. The lecture of the temperature would be processed to be used by the external RX/TX module. Each temperature sensor would be calibrated at a DC bias. This waveform would be used by the receptor when the data from the tag must be processed to have the lecture of the temperature. In this stage of the design,

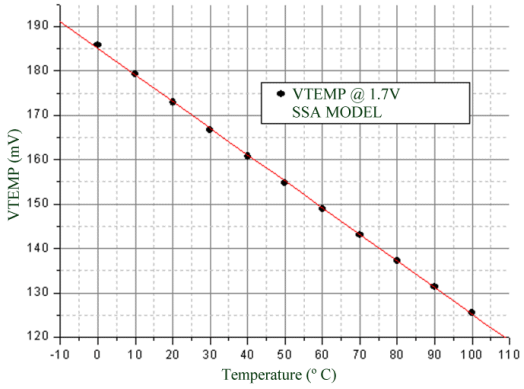

Fig 9. Fit line @ 1,7V for the SSA Case.

to have an approach to the error we have assumed the following procedure. Defined the Vout,max and Vout,min voltages, at the average voltage the calibrated equation would be obtained. If the system is defined to work between Vout,max =1.8 V, and Vout,min = 1.6 V, the reference linear fit waveform is for a bias of 1.7V. In Fig.8, is presented the linear fit in this case, for the typical option (TYP). The fit is VTEMP= BT+A, where A=156,5mV (with an error of 0.1mV), and B= -0.615 mV/ºC, with and error of

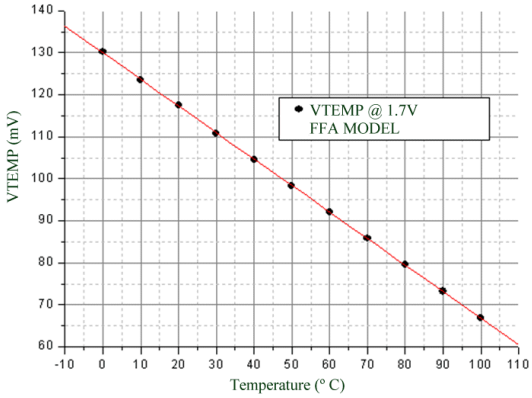

Fig 10. Fit line @ 1,7V for the FFA case.

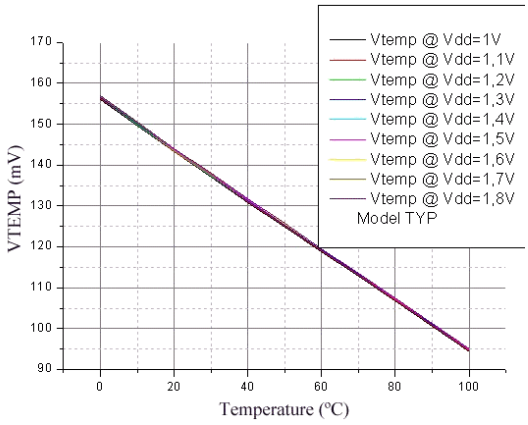

Fig 11. Temperature response with the preregulator @ TYP.

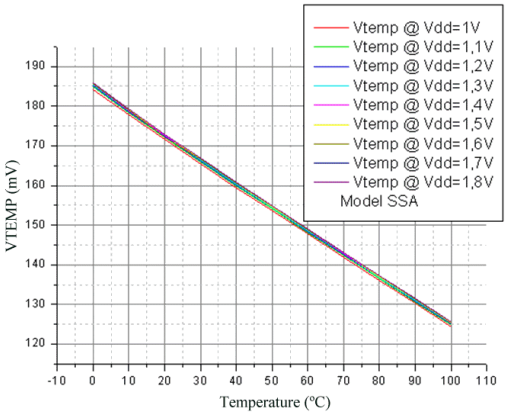

Fig 12. Temperature response with the preregulator @ SSA.

17 µV/ºC, and an R factor of -0.99996. In the case of the slow model (SSA), Fig.9, the fit is VTEMP= BT+A, where A=185,1mV (with an error of 0.19mV), and B= -0.599 mV/ºC, with and error of 3 µV/ºC, and an R factor of -0.99986. In the case of the fast model (FFA), Fig.10, the fit is VTEMP= BT+A, where A=129,9mV (with an error of 0.07mV), and B= -0.632 mV/ºC, with and error of 12 µV/ºC, and an R factor of -0.99998. Then, based on this assumption,

we have done an approach to the error in the lecture of the sensor for the different models. In Fig.11 are represented the waveforms of the temperature sensor for different power supplies, that represent the value of the voltage at the SCAP during the discharge phase, for the typical case (TYP). In the particular case of Vout,max =1.8 V, and Vout,min = 1.6 V, and the reference fit waveform is for a bias of 1.7V, we obtain the lecture error between the reference fit and the extreme waveforms, which are resumed in Table 2.

In Fig.12 are represented the waveforms of the sensor in the case of the (SSA) model, and in Fig.13 for the (FFA) model. The respective errors are presented in Table 3 and 4.

4 Conclusion

In this paper has been presented a first approach to develop a self-powered temperature sensor system based on a commercial Piezoelectric generator, which is based on the Quick Pack QP20W (Midé Technology Corporation, Medford, MA, USA). The voltage applied to the electronics in terms of the solution without the LDO, (in this case the integrated power management and control circuitry, the temperature sensor and the external RX/TX circuit), varies between two values, defined by Vout,max and Vout,min.

A pre-regulator, based on a small and low power LDO, is designed to bias the temperature sensor. This solution has been adopted to minimize the variation of the temperature sensor in the range of lecture, defined by the discharge phase. A complete analysis has been developed. The lecture error of the temperature sensor, in the range of operation between 1.8V to 1.6V, has been analyzed in function of the electrical models, described by the typical (TYP), slow (SSA), and fast (FFA) options.

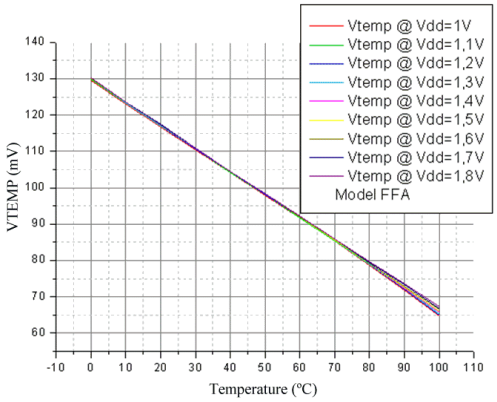

Fig 13. Temperature response with the preregulator @ FFA.

REF	Vdd=1,6V		Vdd=1,8V	
Tª(º C)	*T (ºC)*	*Error ΔT (ºC)*	*T (ºC)*	*Error ΔT (ºC)*
0	-0,14451	**0,14451**	0	**0**
20	19,86982	**0,13018**	19,98537	**0,01463**
40	39,88414	**0,11586**	39,97074	**0,02926**
60	59,89847	**0,10153**	59,95611	**0,04389**
80	79,91279	**0,08721**	79,94148	**0,05852**
100	99,92712	**0,07288**	99,92685	**0,07315**

Table 2. Lecture error for the Typical (TYP) case

REF	Vdd=1,6V		Vdd=1,8V	
T (ºC)	T (ºC)	ΔT (ºC)	T (ºC)	ΔT (ºC)
0	-0,1315	**0,1315**	0,0848	**-0,0848**
20	19,886	**0,1137**	20,0687	**-0,0687**
40	39,9034	**0,0960**	40,0527	**-0,053**
60	59,9217	**0,0783**	60,0367	**-0,037**
80	79,9394	**0,0606**	80,027	**-0,021**
100	99,9571	**0,0429**	100,0046	**-0,005**

Table 3. Lecture error for the Slow (SSA) case

REF	Vdd=1,6V		Vdd=1,8V	
Tª (ºC)	T (ºC)	ΔT (ºC)	T (ºC)	ΔT (ºC)
0	-0,01003	**0,01**	-0,2409	**0,24**
20	19,90767	**0,092**	19,90679	**0,093**
40	39,82536	**0,17**	40,05448	**-0,055**
60	59,74305	**0,26**	60,20218	**-0,20**
70	69,7019	**0,30**	70,27602	**-0,28**
80	79,66075	**0,34**	80,34987	**-0,35**
90	89,6196	**0,38**	90,42371	**-0,42**
100	99,57844	**0,42**	100,49756	**-0,49**

Table 4. Lecture error for the Fast (FFA) case

In the temperature range, from 0ºC to 100ºC, included the worst case; the maximum error is 0.49ºC.

A full integrated circuit is being designed in order to test and check the performances of the presented design.

The oriented application of this system is to sense the temperature in harsh environments or when accessibility is limited to human operators, where a great accuracy it is not necessary.

References:

[1] D.Puccinelli, M.Haenggi, "Wireless sensor networks: applications and challenges of ubiquitous sensing", IEEE Circuits and Systems Magazine, vol.3, no. 3, pp. 19-29, 2005

[2] S.Roundy, D.Steingart, L.Frechette, P.Wright, and J.Rabaey, "Power sources for wireless sensors networks", 1st European Workshop on Wireless Sensors Networks, Berlin, Germany, 2004.

[3] Adilson J.Cardoso, Cesar R.Rodrigues, Rafael S.Pippi, César A.Prior, Felipe C.B.Vieira, "CMOS Energy Harvester Based on al Low-Cost Piezoelectric Acoustic transducer", 1-4244-0173-9/06/$20.00, IEEE 2006.

[4] Christian Sauer, Milutin Stanacevic, Gert Cauwenberghs, Nitish Thakor, "Power Harvesting and Telemetry in CMOS for Implant Devices", IEEE Transactions on Circuits and Systems, December 2005, Vol. 52, No. 12.

[5] J.Brufau, M.Puig, "Piezoelectric polymer model validation applied to mm size micro-robot I-SWARM (intelligent swarm)", Proceedings of the SPIE 2006, vol. 6166, pp. 229-240

[6] J.Yueming, L.Edward. " Design of Low-Voltage bandgap refrence Using Transimpedance Amplifier", IEEE Transactions on Circuits and Systems-II, June 2000, Vol. 47, pp.552-555

[7] Robert Pease, "The Design of Bad-Gap Reference Circuits: Trials and Tribulations". IEEE 1990 Bipolar Circuits and Technology Meeting, pp 214-218, 1990.

[8] Anne-Johan Annema, "Low-Power Bandgap References Featuring DTMOST's", IEEE Journal of Solid-State Circuits, vol.34, No.7, July 1999.

[9] M.Pertijs, K.Makinwa, "A CMOS Temperature Sensor with 3σ Inaccuracy of ± 0.1ºC from -55ºC to 125 ºC", Proceedings of ISSCC 2005, Session 13, Sensors, 13.1, pp.238-240.

[10] Yiming Zhai; Prakash, S.B.; Cohen, M.H.; Abshire, P.A. “Detection of on-chip temperature gradient using a 1.5V low power CMOS temperature sensor” Proceedings of the Circuits and Systems, 2006, pp. 1171-1174. ISCAS 2006. IEEE International Symposium, May 2006.

[11] I.M. Filanovsky, Su Tam Lim, " Temperature sensor applications of diode-connected MOS transistors", Proceedings of the Circuits and Systems, 2002, pp 149-152. ISCAS 2005. IEEE International Symposium , May 2002.

[12] G.A. Rincón-Mora, " Voltage references", IEEE Press, Wiley Interscience, ISBN:0-471-14336-7. 2002.